NUMERICAL EXPERIMENTS WITH SEVERAL TIME DIFFERENCING SCHEMES WITH A BAROTROPIC PRIMITIVE EQUATION MODEL ON A SPHERICAL GRID

George Washington Heburn

NAVAL POSTGRADUATE SCHOOL
Monterey, California

THESIS

NUMERICAL EXPERIMENTS WITH SEVERAL TIME DIFFERENCING SCHEMES WITH A BAROTROPIC PRIMITIVE EQUATION MODEL ON A SPHERICAL GRID

by

George Washington Heburn

Thesis Advisor: G. J. Haltiner
Thesis Advisor: R. T. Williams

MAR 1972

Numerical Experiments With Several Time Differencing Schemes With a Barotropic Primitive Equation Model on a Spherical Grid

by

George Washington Heburn
Lieutenant, United States Navy
B.A.E., Georgia Institute of Technology, 1966

Submitted in partial fulfillment of the
requirements for the degree of

MASTER OF SCIENCE IN METEOROLOGY

from the

NAVAL POSTGRADUATE SCHOOL
March 1972

ABSTRACT

Four time differencing schemes were tested using a barotropic primitive equation model on a spherical staggered grid with an analytic input in order to compare amplitudes, phase speeds, and computation time for each. The methods tested were the leapfrog, Euler-backward, leapfrog-trapezoidal, and Adams-Bashford. One set of experiments was performed using an averaging technique to reduce the effects of gravity waves in the higher latitudes. Another set was performed without the averaging in order to determine the effects of this technique on the solutions.

TABLE OF CONTENTS

LIST OF FIGURES

LIST OF SYMBOLS

A	- Arbitrary constant in the stream function
A_m	- Arbitrary constants for fourier series cosine terms
A_j	- Constant used in the Arakawa averaging method
a	- Earth's radius
B	- Arbitrary constant in the stream function
B_m	- Arbitrary constants for fourier series sine terms
C_m	- Arbitrary constants for fourier series combined terms
c	- Wave speed
d	- Grid increment
D_j	- Constant used in the Arakawa averaging method
$\tilde{D}_j$	- Greatest integer value of D_j
F	- Arbitrary function
f	- Coriolis parameter
g	- Acceleration of gravity
h	- Height of free surface
h^*	- Height of free surface at wind points
$\tilde{h}$	- Height computed by equation (3) in "restorative-iterative" method
h_o	- Height derived from the linear balance equation and used as an "observed" value in the "restorative-iterative" method
i	- Grid index in the x-direction (east-west)
j	- Grid index in the y-direction (north-south)
k_u	- Restoration coefficient for zonal wind
k_v	- Restoration coefficient for meridional wind
k_h	- Restoration coefficient for height
l	- Variable grid index in the x-direction which is dependent on j

m - Wave number

N - Iteration index

n - Degree of the Legrendre function

P_n^m - Legrendre function of order m and degree n

t - Time

u - Zonal wind (x-direction)

uh - $u \times h^*$ at wind points

$(uh)^*$ - uh at mass (height) points

$\widetilde{uh}$ - uh computed by equation (1) in the "restorative-iterative" method

$(uh)_o$ - uh derived from the linear balance equation and used as an "observed" value in the "restorative-iterative" method

v - Meridional wind (y-direction)

vh - $v \times h^*$ at wind points

$(vh)^*$ - vh at mass (height) points

$\widetilde{vh}$ - vh computed by equation (2) in the "restorative-iterative" method

$(vh)_o$ - vh derived from the linear balance equation and used as an "observed" value in the "restorative-iterative" method

x - East-west direction

y - North-south direction

Δt - Time increment

Δx - Distance increment in x-direction

Δy - Distance increment in y-direction

$\Delta\Theta$ - Distance increment in latitudinal direction

$\Delta\lambda$ - Distance increment in longitudinal direction

δ_m - Phase angle for wave number m

Θ - Latitude

λ - Longitude

ν - Angular wave speed

ψ - Stream function

∇ - Del operator (horizontal)

∇^2 - Laplacian operator (horizontal)

ACKNOWLEDGEMENTS

The author wishes to express his thanks to Dr. G. J. Haltiner for his encouragement to undertake this project, Dr. R. T. Williams for his patient guidance without which this project would never have been completed, Dr. F. J. Winninghoff for providing the original program, and finally the W. R. CHURCH COMPUTER CENTER of the NAVAL POSTGRADUATE SCHOOL for providing the many hours of computer time required to complete this project.

I. INTRODUCTION

In the field of operational numerical weather prediction, the trend, in recent years, has been toward the development of sophisticated global prediction models. This has been made possible by the rapid expansion of computing capacity and developments related to general circulation research.

The purpose of this study was to examine various time differencing methods, using a barotropic primitive equations model on a global staggered grid. A spherical harmonic analytic stream function was used for the initial conditions. By using an analytic initial condition, errors in real data observations and analysis, which are unavoidable in practical dynamical prediction, were eliminated.

The objective was to compare the time required for computation, amplitudes, and phase speeds for each of the time differencing schemes.

II. BAROTROPIC PRIMITIVE EQUATIONS MODEL

Time differencing experiments were performed using the free surface barotropic primitive equations. The integrations were carried out on the sphere using the difference method of the Arakawa type which was developed by Winninghoff (1971).

A. PRIMITIVE EQUATIONS

The primitive equations, in spherical coordinates and in flux form, for this model are:

$$\frac{\partial (uh)}{\partial t} = -\frac{1}{a \cos \Theta}\left[\frac{\partial (uuh)}{\partial \lambda} + \frac{\partial (uvh \cos \Theta)}{\partial \Theta}\right] + \frac{uvh \tan \Theta}{a} + fvh - \frac{h}{a \cos \Theta}\frac{\partial (gh)}{\partial \lambda} \qquad (1)$$

$$\frac{\partial (vh)}{\partial t} = -\frac{1}{a \cos \Theta}\left[\frac{\partial (vuh)}{\partial \lambda} + \frac{\partial (vvh \cos \Theta)}{\partial \Theta}\right] - \frac{uuh \tan \Theta}{a} + fuh - \frac{h}{a}\frac{\partial (gh)}{\partial \lambda} \qquad (2)$$

$$\frac{\partial (h)}{\partial t} = -\frac{1}{a \cos \Theta}\left[\frac{\partial (uh)}{\partial \lambda} + \frac{\partial (vh \cos \Theta)}{\partial \Theta}\right] \qquad (3)$$

Equations (1) and (2) are, respectively, the zonal and meridional momentum equations, and equation (3) is the continuity equation.

B. GRID

The spatial finite differencing was performed on a staggered, spherical grid. The wind and height variables were carried at alternate points (see Fig. 1) with height only at the poles. The latitudinal and longitudinal grid increments were five degrees. This gives 2560 points (72 x 35) over the globe, with wind and height carried at 1260 points each.

```
                     h (North Pole)

      u,v   h   u,v   h   . . . . . . . .   h
       h   u,v   h   u,v  . . . . . . . .  u,v
       .
       .
       .
       .
       .
      u,v   h   u,v   h   . . . . . . . .   h
  ↑    h   u,v   h   u,v  . . . . . . . .  u,v
  j   u,v   h   u,v   h   . . . . . . . .   h
    i →            h (South Pole)
```

FIGURE 1. LOCATION OF VARIABLES

C. SPATIAL FINITE DIFFERENCING

Spatial differencing of the Arakawa (1966) type was used which eliminates the spurious energy growth which can occur with standard finite difference approximations to the nonlinear advection terms. The difference equations used here for this model are:

$$\frac{\Delta(uh)_{ij}}{\Delta t} = -\frac{1}{a\cos\Theta_j}\left[\frac{(u_{ij}+u_{i+1j})(uh)^*_{i+\frac{1}{2}j}-(u_{ij}+u_{i-1j})(uh)^*_{i-\frac{1}{2}j}}{2\Delta\lambda}\right.$$

$$\left.+\frac{(u_{ij}+u_{ij+2})(vh)^*_{ij+1}\cos\Theta_{j+1}-(u_{ij}+u_{ij-2})(vh)_{ij-1}\cos\Theta_{j-1}}{2\Delta\Theta}\right]$$

$$+\frac{u_{ij}(vh)_{ij}\tan\Theta_j}{a} + f_j(vh)_{ij} - \frac{gh^*_{ij}}{a\cos\Theta_j}\left[\frac{h_{ij}-h_{i-1j}}{\Delta\lambda}\right] \quad (4)$$

$$\frac{\Delta(vh)_{ij}}{\Delta t} = -\frac{1}{a\cos\Theta_j}\left[\frac{(v_{ij}+v_{i+1j})(uh)^*_{i+\frac{1}{2}j}-(v_{ij}+v_{i-1j})(uh)^*_{i-\frac{1}{2}j}}{2\Delta\lambda}\right.$$

$$\left.+\frac{(v_{ij}+v_{ij+2})(vh)^*_{ij+1}\cos\Theta_{j+1}-(v_{ij}+v_{ij-2})(vh)^*_{ij-1}\cos\Theta_{j-1}}{2\Delta\Theta}\right]$$

$$-\frac{u_{ij}(uh)_{ij}\tan\Theta_j}{a} - f_j(uh)_{ij} - \frac{gh^*_{ij}}{a}\left[\frac{h_{\ell-1\ j-1}-h_{\ell-1\ i-1}}{\Delta\Theta}\right] \quad (5)$$

$$\frac{\Delta h_{ij}}{\Delta t} = -\frac{1}{a\cos\Theta_j}\left[\frac{(uh)_{i+1j}-(uh)_{i-1j}}{\Delta\lambda}\right.$$

$$\left.+\frac{(vh)_{\ell j+1}\cos\Theta_{j+1}-(vh)_{\ell j-1}\cos\Theta_{j-1}}{\Delta\Theta}\right] \quad (6)$$

where

$$(uh)_{ij} \equiv u_{ij}h^*_{ij}$$

and

$$(vh)_{ij} \equiv v_{ij}h^*_{ij}$$

where

$$h^*_{ij} \equiv \tfrac{1}{2}(h_{ij}+h_{i-1j}) - \tfrac{1}{16}(h_{i+1j}-h_{ij}-h_{i-1j}+h_{i-2j})$$

which is a second order, one-dimensional Bessel's interpolation scheme with $p = \frac{1}{2}$.

Similarly

$$(uh)^{*}_{i+\frac{1}{2}j} \equiv \tfrac{1}{2}[(uh)_{ij}+(uh)_{i+1j}] - \tfrac{1}{16}[(uh)_{i+2j}-(uh)_{i+1j}$$

$$-(uh)_{ij}+(uh)_{i-1j}]$$

and

$$(vh)^{*}_{ij+1} \equiv \tfrac{1}{2}[(vh)_{ij+1}+(vh)_{i-1j}] - \tfrac{1}{16}[(vh)_{i+1j+1}-(vh)_{ij+1}$$

$$-(vh)_{i-1\ j+1}+(vh)_{i-2\ j+1}]$$

Originally, all the interpolated, starred quantities were derived using a two-dimensional linear interpolation. This method was found to introduce a 2d-wave which in certain areas was an order of magnitude greater in amplitude than the zonal wave used for the experiments.

Figure 2 shows the indexing convention used for the mass and wind variables. The index l in equations (5) and (6) was i if j was odd and i + 1 if j was even.

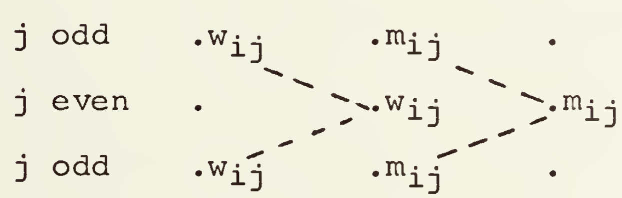

FIGURE 2. GRID INDEXING

III. TIME DIFFERENCING METHODS

Four time differencing methods were used to evaluate the phase angle and amplitude errors of each method. The errors were evaluated by comparison to an analytic solution to the non-divergent barotropic vorticity equation.

The four methods tested were the leapfrog, Euler-backward, leapfrog-trapezoidal, and Adams-Bashford schemes. Two tests were made with each method.

The first set of tests used time increments of fifteen minutes for the first three methods and ten minutes for the Adams-Bashford scheme.

These time steps were possible, even though the i grid distance at 85° N and S is only 40 km, because of a procedure, used by Arakawa (Langlois and Kwok, 1969) to average the effects of high frequency inertial gravity waves in the zonal direction.

The averaging technique involved a coefficient

$$A_j \equiv .125(D_j - 1)/\tilde{D}_j \tag{7}$$

where

$$D_j = \frac{1}{\cos \Theta_j}$$

and $\tilde{D}_j$ was the greatest integer value of D_j.

The uh terms in equation (3) and in the advective terms of equation (1) and (2) were replaced by

$$(uh)^1_{ij} = (uh)_{ij} + A_j[(uh)_{i+1j} + (uh)_{i-1j} - 2(uh)_{ij}]$$

$$\text{For } 1 < D_j < 2 \tag{8}$$

and

$$(uh)^{N}_{ij} = (uh)^{N-1}_{ij}+A_{j}[(uh)^{N-1}_{i+1j}+(uh)^{N-1}_{i-1j}-2(uh)^{N-1}_{ij}] \quad \text{for } N \le D_j < N+1 \qquad (9)$$

Similarly h in the pressure gradient term in equation (1) was replaced by

$$h^{1}_{ij} = h_{ij}+A_{j}[h_{i+1j}+h_{i-1j}-2h_{ij}] \quad \text{for } 1<D_j<2 \qquad (10)$$

and

$$h^{N}_{ij} = h^{N-1}_{ij}+A_{j}[h^{N-1}_{i+1j}+h^{N-1}_{i-1j}-2h^{N-1}_{ij}] \quad \text{for } N \le D_j<N+1 \qquad (11)$$

No averaging was done if $D_j \le 1$.

The second set of tests were run without using the averaging technique. Thus to remain within the von Neumann linear computational stability criterion (Haltiner, 1971), a 2.5-minute time step was used. The two sets of tests were run in order to determine the effects of the averaging technique on the solutions.

A. LEAPFROG

The leapfrog method is a centered time differencing scheme which is conditionally stable for $\frac{c\Delta t}{\Delta x} < 1$. The finite difference equation is:

$$F^{t+1} = F^{t-1} + 2\Delta t \frac{\partial F^{t}}{\partial t} \qquad (12)$$

Since this method has three time levels, it has both a physical and a computational mode.

B. EULER-BACKWARD

The Euler-backward method is a two-step iterative scheme which is conditionally stable for $\frac{c\Delta t}{\Delta x} < 1$. The difference equations are:

$$F^* = F^t + \Delta t \frac{\partial F^t}{\partial t}$$

$$F^{t+1} = F^t + \Delta t \frac{\partial F^*}{\partial t} \qquad (13)$$

Since the Euler-backward method has just two time levels it has only a physical mode.

C. LEAPFROG-TRAPEZOIDAL

The leapfrog-trapezoidal is another two-step iterative scheme which is conditionally stable for $\frac{c\Delta t}{\Delta x} < \sqrt{2}$.

The difference equations are:

$$F^* = F^{t-1} + 2\Delta t \frac{\partial F^t}{\partial t}$$

$$F^{t+1} = F^t + \frac{\Delta t}{2}\left(\frac{\partial F^*}{\partial t} + \frac{\partial F^t}{\partial t}\right) \qquad (14)$$

Since this method, like the leapfrog, has three time levels, it also has both a physical and a computational mode.

D. ADAMS-BASHFORD

The Adams-Bashford method used was the one examined by Lilly (1965).

The difference equation is:

$$F^{t+1} = F^t + \Delta t \left(\frac{3}{2}\frac{\partial F^t}{\partial t} - \frac{1}{2}\frac{\partial F^{t-1}}{\partial t}\right) \qquad (15)$$

This method has three time levels, thus it has both a computational and a physical mode. The method is unstable but has some desirable features. The computational mode tends to damp and the rate of erroneous amplification of the physical mode is small if Δt is small.

IV. INITIAL CONDITIONS

The initial velocity and height fields for these experiments were derived from a stream function which is a solution to the non-divergent barotropic vorticity equation. The stream function used was examined by Gates (1962) and Neamtan (1946), which is:

$$\psi = A \sin(m\lambda - \nu t)\, P_n^m (\sin\Theta) - B\, a^2 \sin\Theta + C\, P_n (\sin\,\Theta) \qquad (16)$$

A reasonable meteorological pattern was obtained from equation (16) by selecting

$C = 0$

$A = 1000\ m^2\ sec^{-1}$

The constant B was related to the angular wave speed by

$$\frac{\nu}{m} = B\,\frac{n(n+1)-2}{n(n+1)} - \frac{2\Omega}{n(n+1)} \qquad (17)$$

For wave number 6 and, with n = 7 for convenience, $\frac{\nu}{m} = 20°$ long. per day

$B = 6.8905 \times 10^{-6}\ sec^{-1}$

The stream function then became

$$\psi = -279.68 \times 10^{-6} \sin\Theta + 136.65 \times 10^{-6} \sin(6\lambda - \nu t) \sin\Theta \cos^6\Theta \quad m^2 sec^{-1} \qquad (18)$$

Since these experiments were performed using a free surface barotropic primitive equations model which allows divergence, equation (17) was satisfied only approximately. Rossby (1939) has shown that the presence of divergence in a barotropic atmosphere will slow up the rate of wave propagation, especially for small values of wave number m.

The initial wind field was a non-divergent wind given by

$$u = -\frac{\partial\psi}{\partial g} = -\frac{1}{a}\frac{\partial\psi}{\partial\Theta} \tag{19}$$

$$v = \frac{\partial\psi}{\partial x} = \frac{1}{a\cos\Theta}\frac{\partial\psi}{\partial\lambda} \tag{20}$$

The initial height field was derived by solving the linear balance equation

$$\nabla^2 h = \frac{1}{g}\left[f\nabla^2\psi + \nabla\psi\cdot\nabla f\right] \tag{21}$$

where

$$\nabla^2 = \frac{1}{a^2}\left[\frac{1}{\cos^2\Theta}\frac{\partial^2}{\partial\lambda^2} + \frac{1}{\cos\Theta}\frac{\partial}{\partial\Theta}\left(\cos\Theta\frac{\partial}{\partial\Theta}\right)\right]$$

and

$$\nabla = \left(\frac{1}{a\cos\Theta}\frac{\partial}{\partial\lambda}, \frac{1}{a}\frac{\partial}{\partial\Theta}\right)$$

Equation (21) was solved by the following relaxation scheme:

$$h_{ij}^{N+1} = h_{ij}^{N} + R_{ij} \tag{22}$$

where

$$R_{ij} = \frac{.9}{\left(\cos\Theta_j + \frac{1}{\cos\Theta_j}\right)}\left[(\cos\Theta_j - d\sin\Theta_j)h_{ij+2} + (\cos\Theta_j + d\sin\Theta_j)h_{ij-2}\right.$$

$$\left. + \frac{(h_{i+1j}+h_{i-1j})}{\cos\Theta_j} - 2\left(\cos\Theta_j + \frac{1}{\cos\Theta_j}\right)h_{ij} - \frac{\cos\Theta_j(2d)^2}{g}(f\nabla^2\psi + \nabla\psi\cdot\nabla f)\right] \tag{23}$$

with a relaxation tolerance of .1 meters.

One experiment, using the leapfrog scheme for time differencing, was performed with the "restorative-iterative" initialization method developed by Winninghoff (1971). This method involved using the Euler-backward time differencing scheme to alternately step forward and backward six times. After each iteration of equations (1), (2), and (3) the following restoration was added:

$$\begin{aligned} (uh)_{ij} &= (1-k_u)\ (\widetilde{uh})_{ij} + k_u(uh)_o \\ (vh)_{ij} &= (1-k_v)\ (\widetilde{vh})_{ij} + k_v(vh)_o \\ h_{ij} &= (1-k_h)\ \widetilde{h}_{ij} + k_h h_o \end{aligned} \tag{24}$$

where the k's are functions of latitude. k_u and k_v were .5 from latitude 20° S to 20° N, 0 from 40° N and S to the poles, and a linear variation between 0 and .5 between latitude 20° and 40°. k_h was .5 from 40° N and S to the poles, 0 between 20° S and 20° N, and a linear variation between 20° and 40°.

V. WAVE ANALYSIS METHOD

To calculate the phase angles and amplitudes, a fourier analysis was performed at each five degrees of latitude around the latitude circle. The fourier series was expressed as follows:

$$F(x) = A_o + \sum_m (A_m \cos mx + B_m \sin mx)$$

$$= C_o + \sum_m C_m \cos (mx - \delta_m)$$

where

$$C_m = \frac{B_m}{\sin(\delta_m)} = \frac{A_m}{\cos(\delta_m)}$$

and

$$\delta_m = \tan^{-1} \frac{B_m}{A_m}$$

Since the input stream function involved only wave number six and a mean height, only C_o, C_6, and δ_6 values were extracted from the fourier analysis.

VI. RESULTS

All the experiments performed with the Arakawa averaging technique showed a considerable tilt backward at high latitudes in the phase propagation of the wave. This is to be expected since the smoothing of the gradients in the technique tends to slow down the rate of propagation. Gates (1959) has shown that, as the wavelength and Δx decrease proportionally, the phase speed of the wave remains constant, and also that if the wavelength decreases and Δx remains constant, the phase speed will decrease relative to the exact value. In this model, the Arakawa averaging technique gives an effective Δx which is comparable to that at low latitudes, thus as the wavelength decreased toward the poles the phase speed also decreased.

The result of this differential movement was to cause, eventually, the formation of closed highs and lows at the higher latitudes which propagated equatorward. It is believed that this instability is possible due to nonlinear effects introduced after the field ceased to be harmonic in the latitudinal direction.

The amplitudes in all the experiments showed a tendency to decrease at latitudes below 45° and increase above 45°. The mean height also tended to increase at the higher latitude (75° and above). These amplitude variations are also believed to be caused by the nonlinear effects. All the methods, except the Euler-backward, had small amplitude gravity waves propagating with about a ten hour period.

Table I shows the comparison of the time required for a 120-hour forecast using each of the four methods. It also gives a comparison of the initial twenty-four phase speed for selected latitudes.

TABLE I

Time Differencing Method	Time Required 120hr Forecast	Phase Speed for Initial 24hrs Equator	30°	60°	75°
Leapforg	32	14.0	10.7	1.7	-11.3
Euler-Backward	57	13.3	11.2	1.5	-9.7
Leapfrog-Trapezoidal	58	13.7	10.8	1.5	-11.5
Adams-Bashford	46	14.3	10.8	1.8	-11.2

Note: Time in minutes
Phase speed in degrees longitude per day

The experiments performed without the averaging technique still showed a slight tendency to tilt backwards at the higher latitudes. This was not expected and was believed to have been caused by truncation errors due to special treatment near the poles using only a second-order difference approximation for the derivatives. This belief was based on the fact that the input stream function does not vary linearly near the poles, which caused problems earlier in the interpolation for $(uh)^*$ and h^*.

Table II gives a relative comparison of the time required by each method using a 2.5-minute time step.

TABLE II

Time Differencing Method	Time Required in Minutes
Leapfrog	40 min. for a 32 hr. forecast
Euler-Backward	70 min. for a 30 hr. forecast
Leapfrog-Trapezoidal	70 min. for a 29 hr. forecast
Adams-Bashford	40 min. for a 32 hr. forecast

A. RESULTS OF INDIVIDUAL EXPERIMENTS USING THE AVERAGING TECHNIQUE

Experiment 1. This experiment was performed using the leapfrog time differencing method. Figure 3 shows the phase angles as a function of latitude at twelve-hour intervals out to thirty-six hours and Fig. 8a shows phase angles at twenty-four hour intervals out to 120 hours. The amplitudes for wave number six and the mean heights are shown in Fig. 13 for selected latitudes.

Experiment 2. The second experiment was performed using the leapfrog scheme and the "restorative-iterative" initialization method. This experiment was performed to see if the tilt of the phase lines could be reduced by letting the mass and wind fields "adjust" before performing the integrations. As can be seen in Fig. 4, the tilt was not reduced.

Experiment 3. The Euler-backward method was used for this experiment. The phase curves are shown in Figs. 5 and 8b. The mean height and wave number six amplitudes are shown in Fig. 14. It should be noted that the gravity waves present in the other three methods are effectively damped out with this method.

Also the maximum variations in amplitudes, which are approximately equal for the other three methods, are slightly less since this scheme tends to damp all waves.

Experiment 4. This experiment was performed using the leapfrog-trapezoidal method. Figures 6 and 8c show the phase angles vs latitude curves. The amplitudes are shown in Fig. 15. The largest gravity wave amplitudes were observed using this method.

Experiment 5. The last experiment using the Arakawa averaging scheme was performed using the Adams-Bashford method. Figures 7 and 8d show the phase relationships and Fig. 16 and amplitudes. There was very little difference in the results between this method and the leapfrog, except for the time required, see Table I, for the integrations.

B. RESULTS OF INDIVIDUAL EXPERIMENTS WITHOUT THE AVERAGING TECHNIQUE

Experiment 6. This experiment, like the first experiment, was performed using the leapfrog scheme. The time step was reduced from 15 minutes to 2.5 minutes. The phase angle profiles are shown in Fig. 9 for zero, twelve, and twenty-four hours.

Experiment 7. This experiment was the same as experiment 3, except Δt was 2.5 minutes. The phase angle results are shown in Fig. 10.

Experiment 8. This experiment was the same as experiment 4 with the exception of Δt, which was reduced to 2.5 minutes. The phase profiles are shown in Fig. 11.

Experiment 9. The same time differencing method was used as in experiment 5. The time increment was reduced from 10 minutes to 2.5 minutes. Figure 12 shows the phase relationships for this experiment.

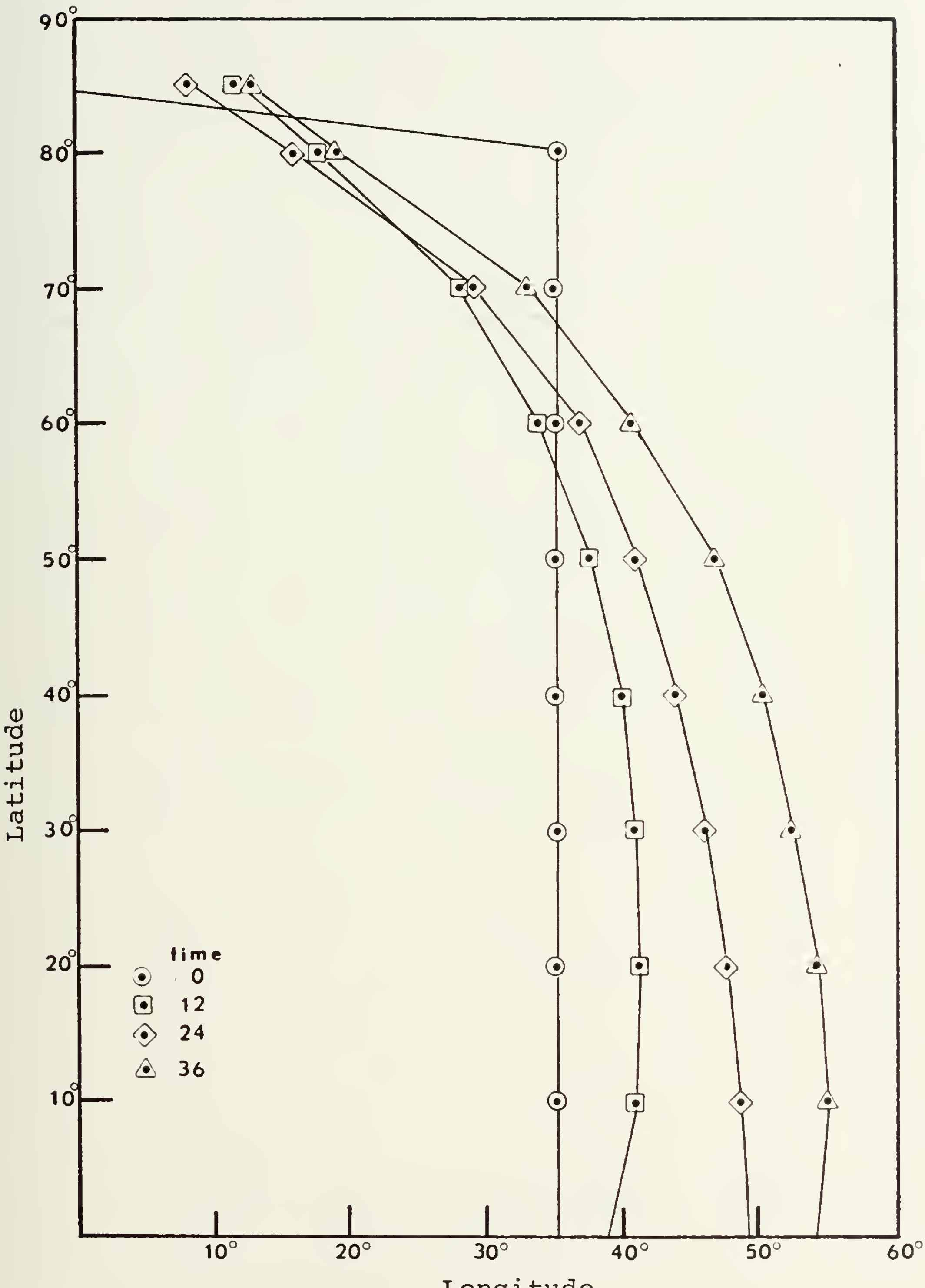

FIGURE 3. PHASE ANGLE VS LATITUDE USING THE LEAPFROG SCHEME WITH THE ARAKAWA AVERAGING.

Note: The input height field was constant at 85° lat. The phase angle at that latitude is the result of truncation errors in the fourier analysis.

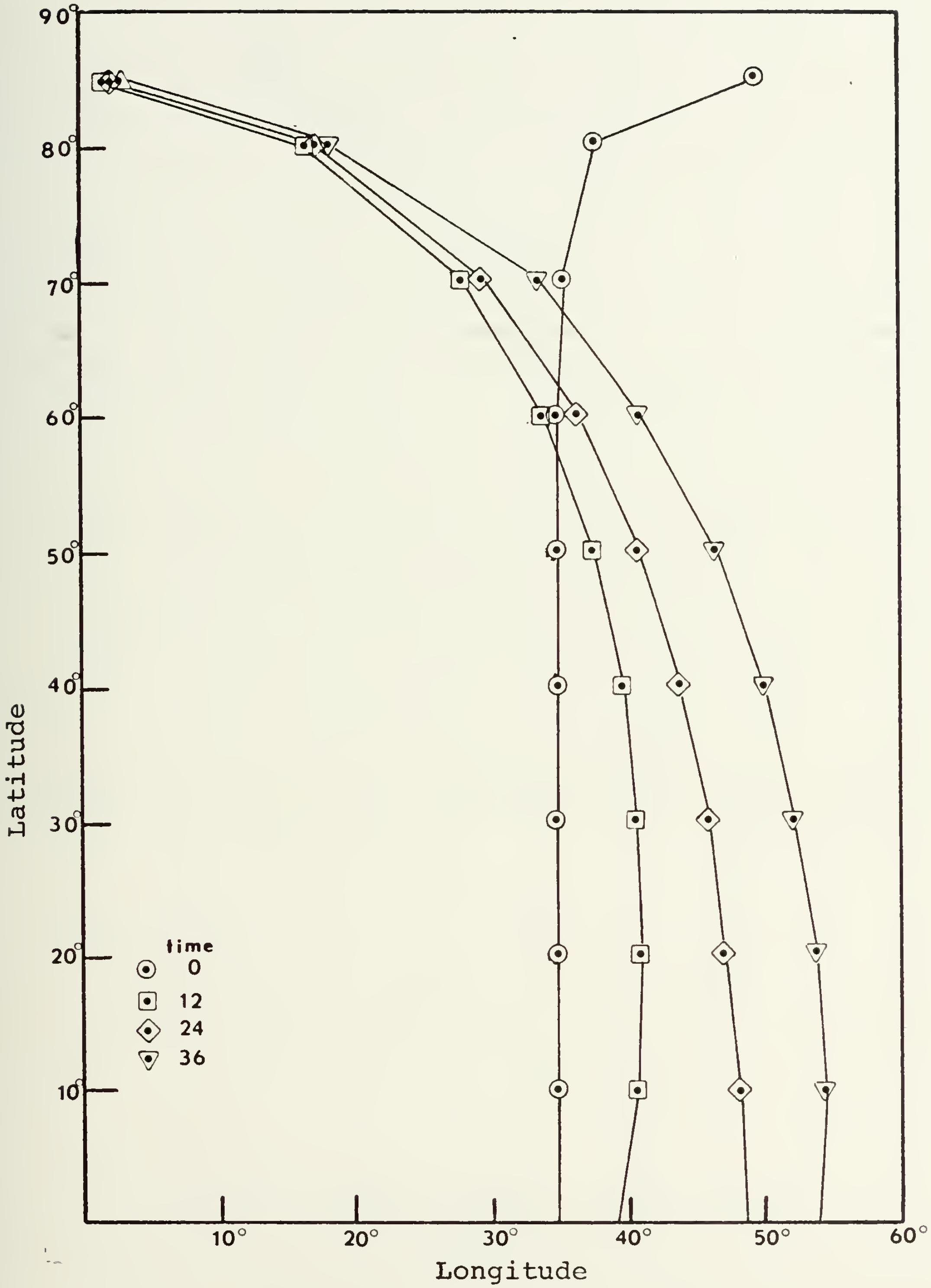

FIGURE 4. PHASE ANGLE VS LATITUDE USING THE LEAPFROG SCHEME WITH THE ARAKAWA AVERAGING AND WINNINGHOFF'S "RESTORATIVE-ITERATIVE" INITIALIZATION.

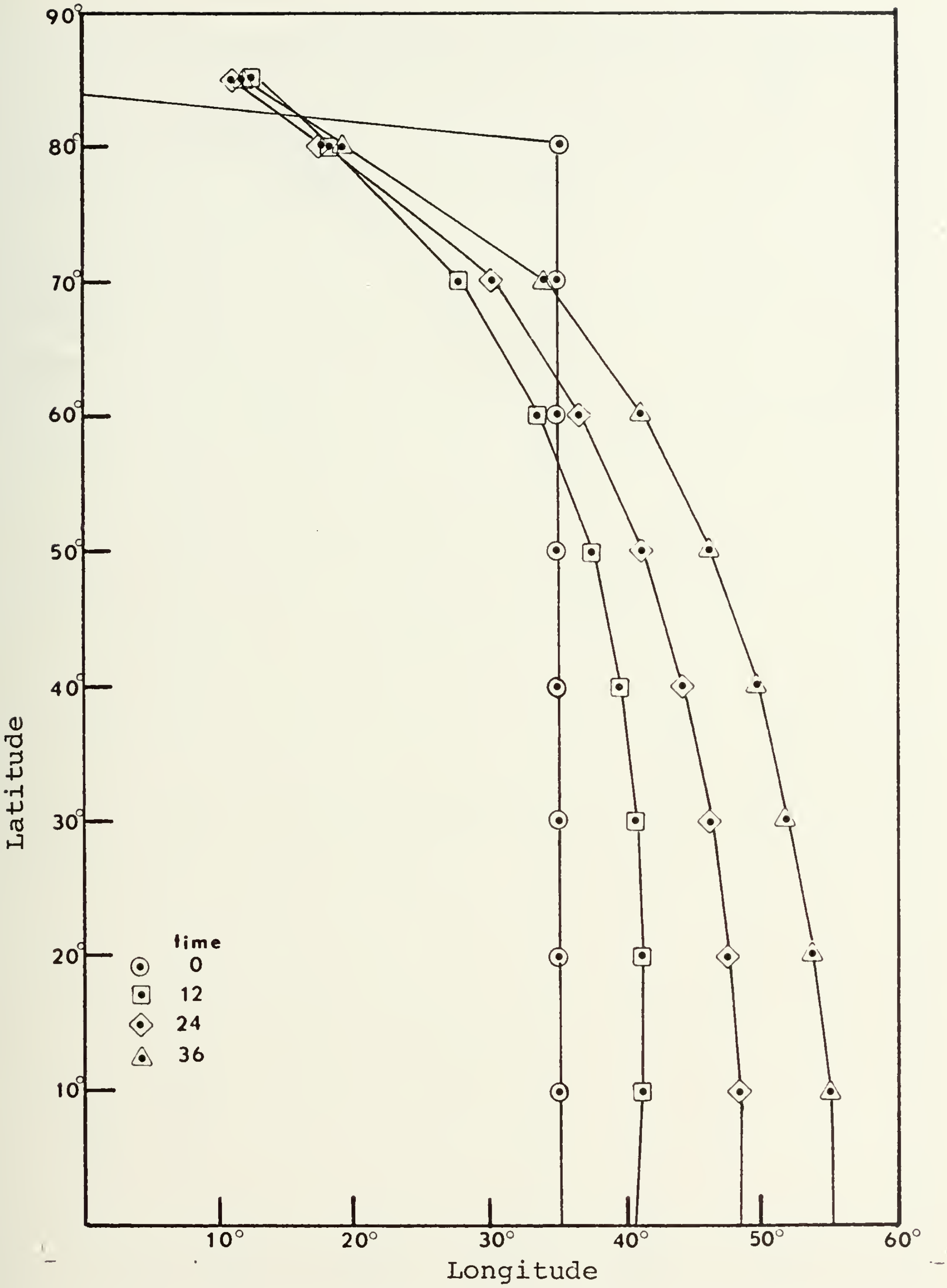

FIGURE 5. PHASE ANGLE VS LATITUDE USING THE EULER-BACKWARD SCHEME WITH THE ARAKAWA AVERAGING.

See note on Fig. 3.

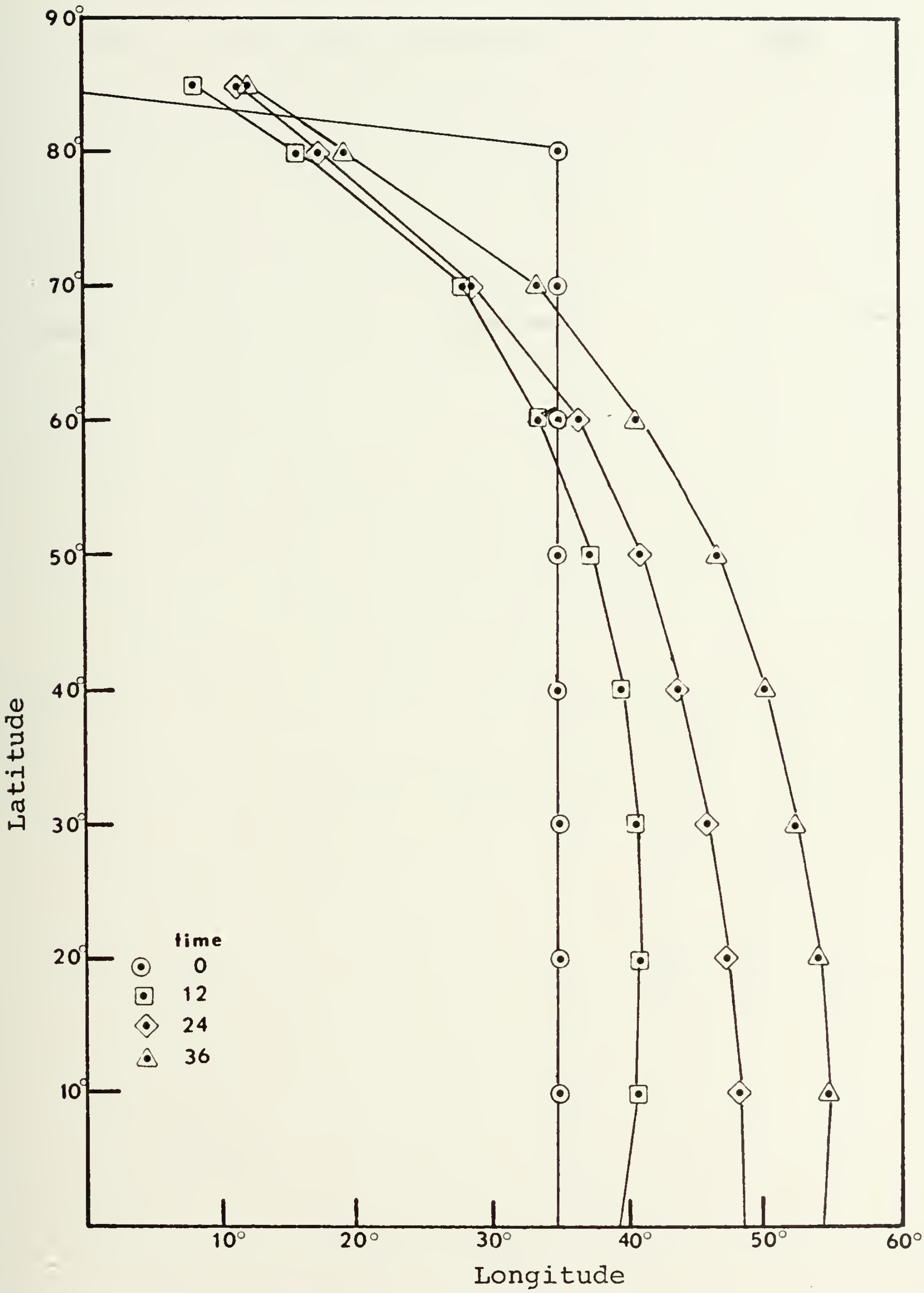

FIGURE 6. PHASE ANGLE VS LATITUDE USING THE LEAPFROG-TRAPEZOIDAL SCHEME WITH THE ARAKAWA AVERAGING.

See note on Fig. 3.

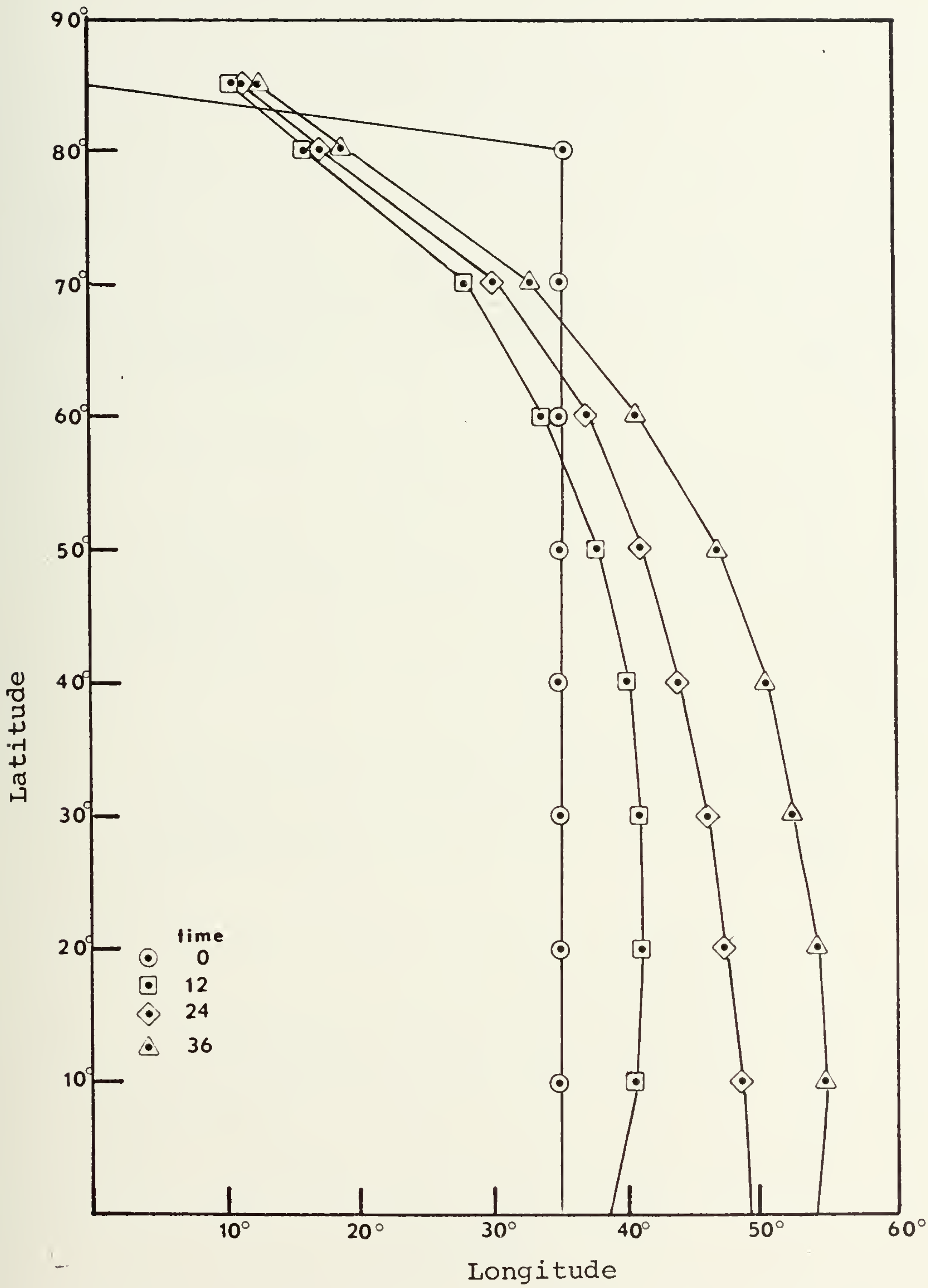

FIGURE 7. PHASE ANGLE VS LATITUDE USING THE ADAMS-BASHFORD SCHEME WITH THE ARAKAWA AVERAGING.

See note on Fig. 3.

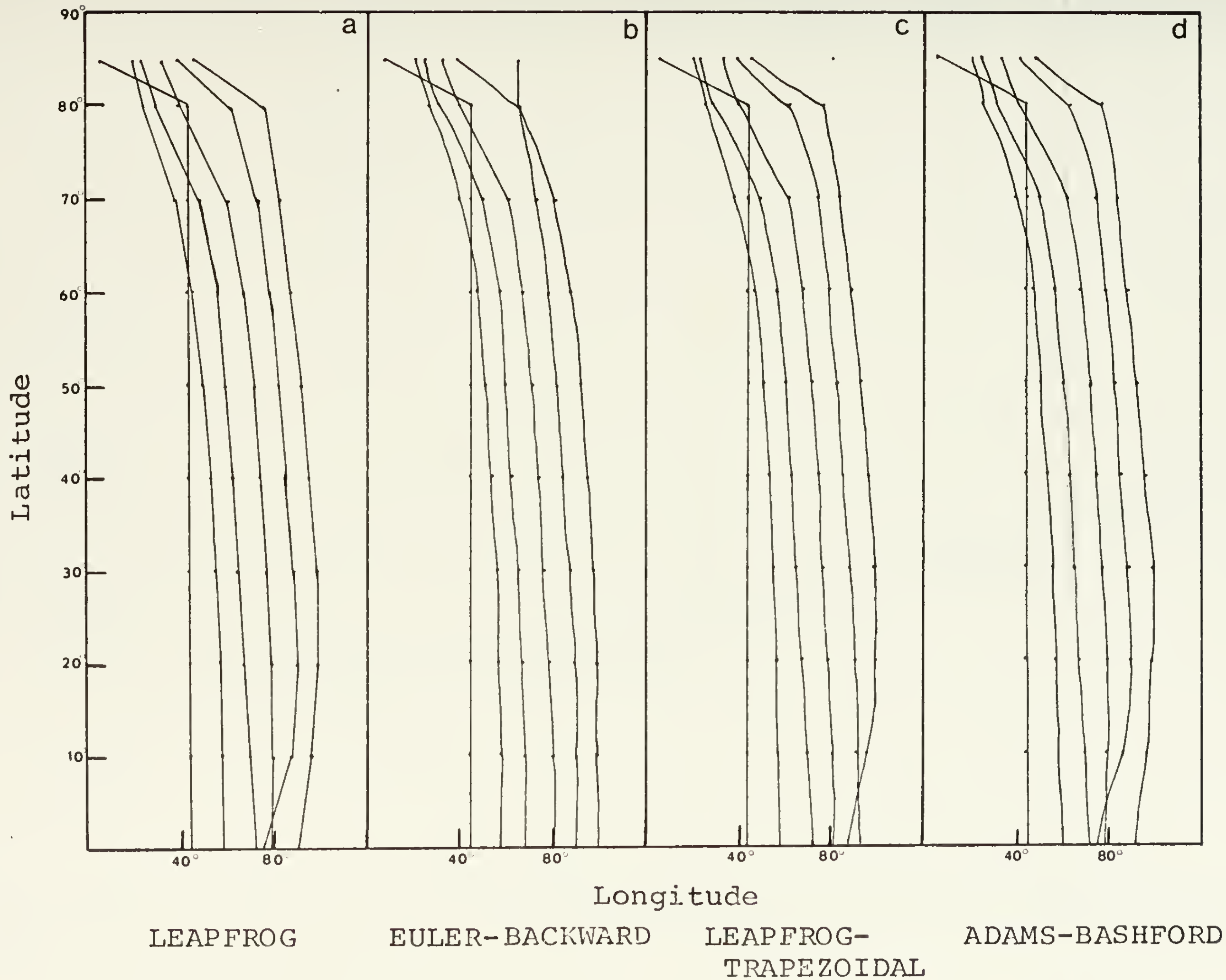

FIGURE 8. PHASE ANGLE VS LATITUDE FOR ALL FOUR SCHEMES WITH THE ARAKAWA AVERAGING AT 24-HOUR INTERVALS OUT TO 120 HOURS.

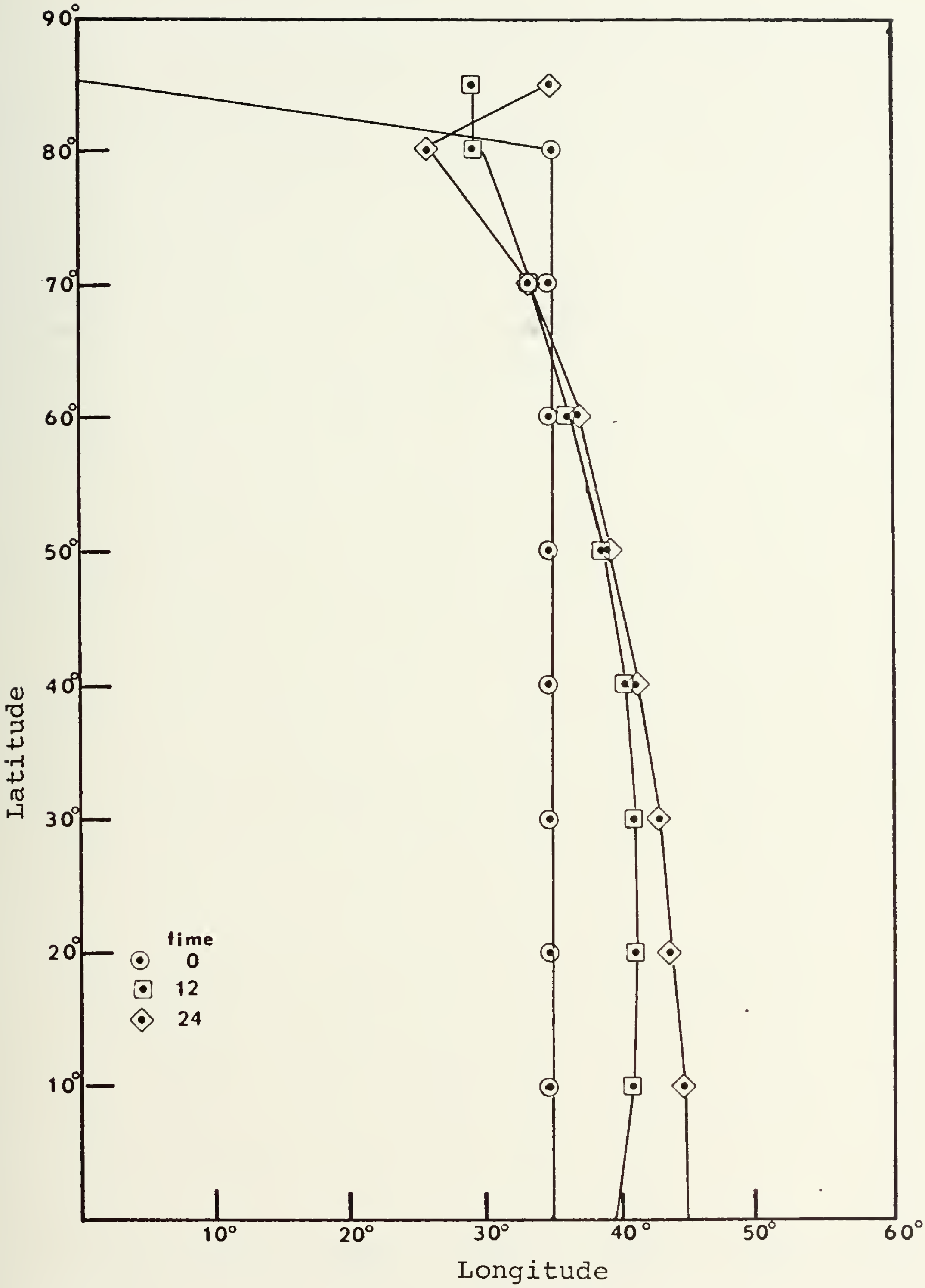

FIGURE 9. PHASE ANGLE VS LATITUDE USING THE LEAPFROG SCHEME WITHOUT AVERAGING.

See note on Fig. 3.

This 24 hour movement appears to be wrong compared to the averaging case but time did not permit a re-run to verify this movement.

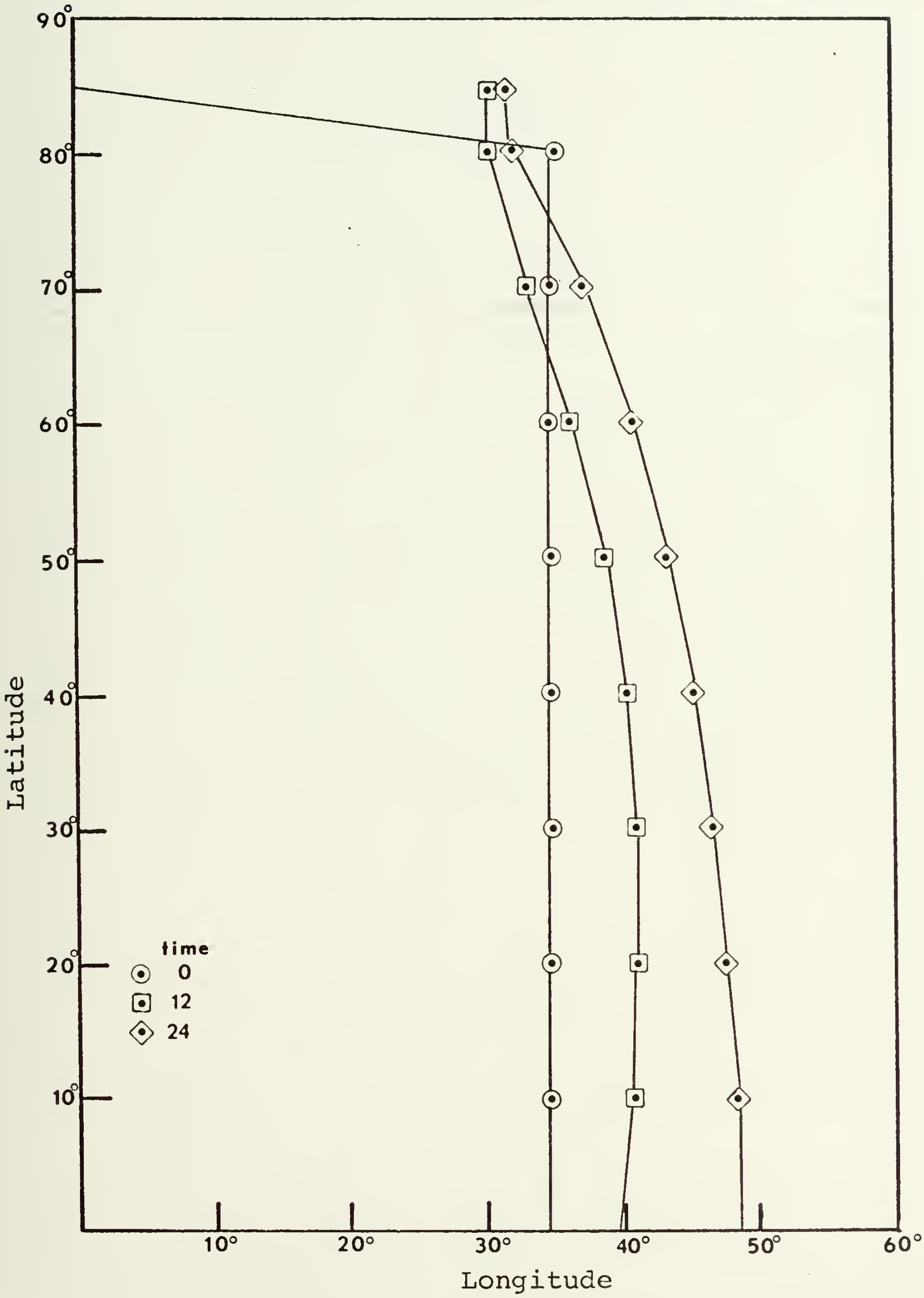

FIGURE 10. PHASE ANGLE VS LATITUDE USING THE EULER-BACKWARD SCHEME WITHOUT AVERAGING.

See note on Fig. 3.

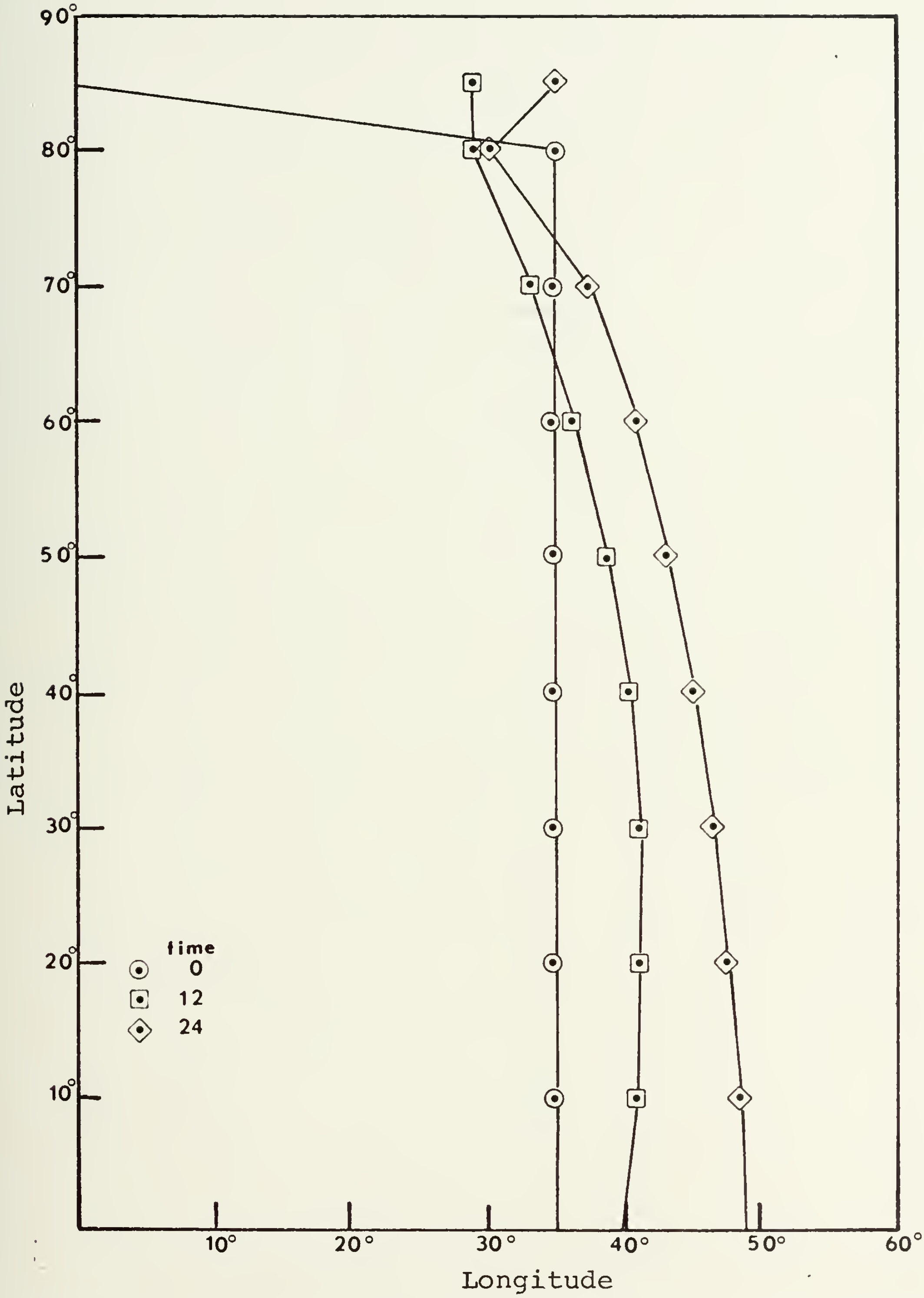

FIGURE 11. PHASE ANGLE VS LATITUDE USING THE LEAPFROG-TRAPEZOIDAL SCHEME WITHOUT AVERAGING.

See note on Fig. 3.

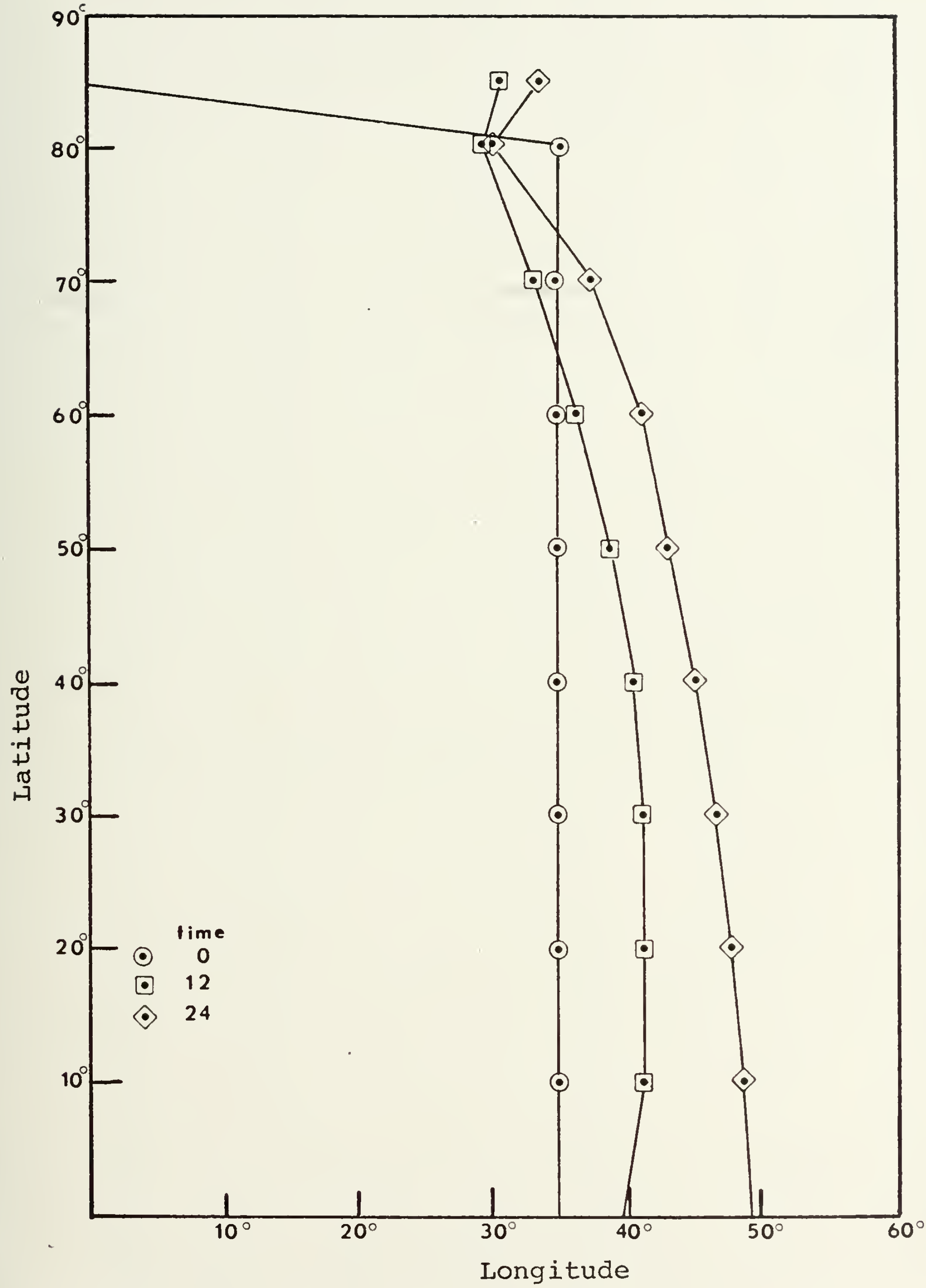

FIGURE 12. PHASE ANGLE VS LATITUDE USING THE ADAMS-BASHFORD SCHEME WITHOUT AVERAGING.

See note on Fig. 3.

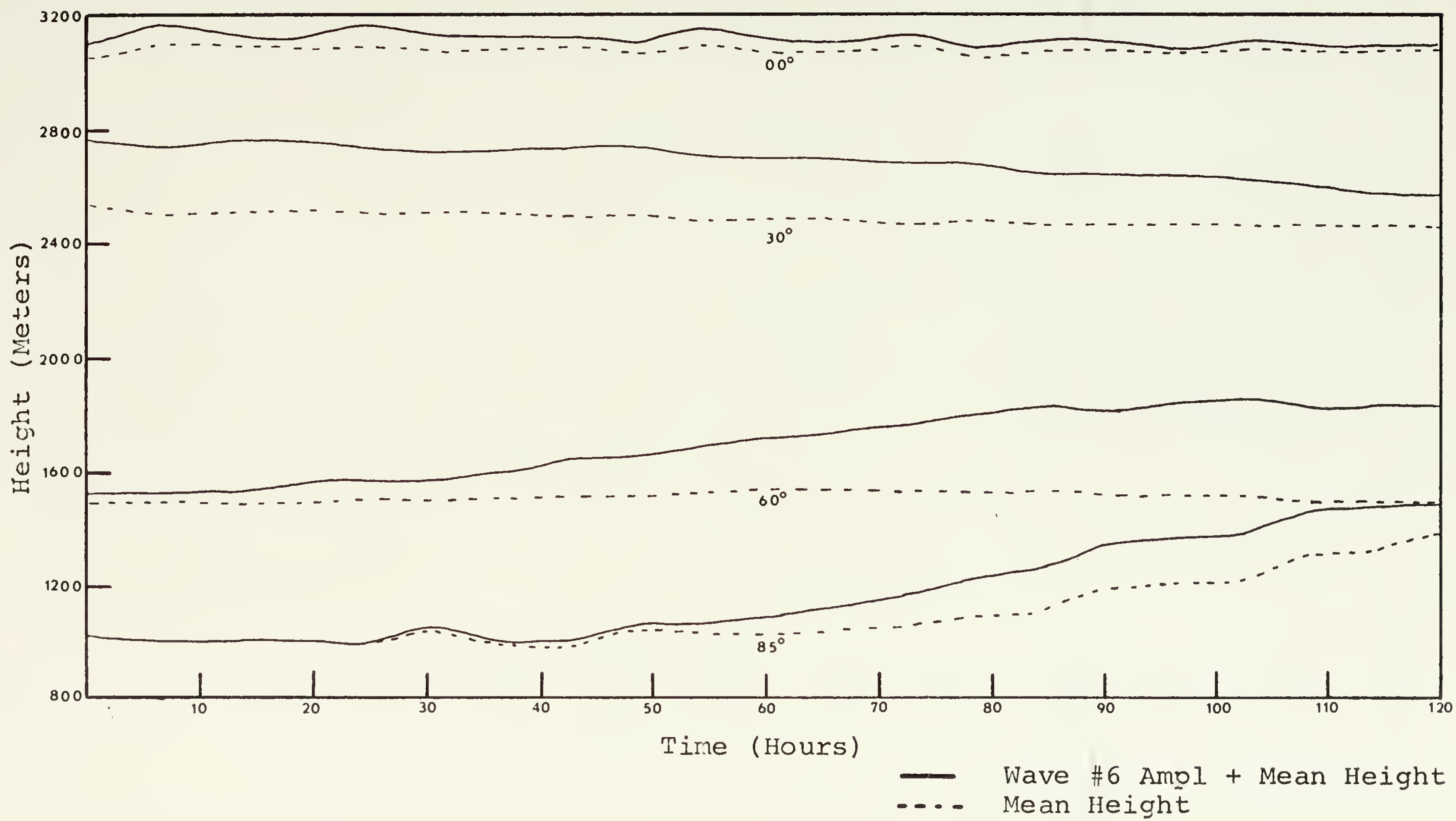

FIGURE 13. AMPLITUDE VS TIME FOR SELECTED LATITUDES USING THE LEAPFORG SCHEME WITH AVERAGING.

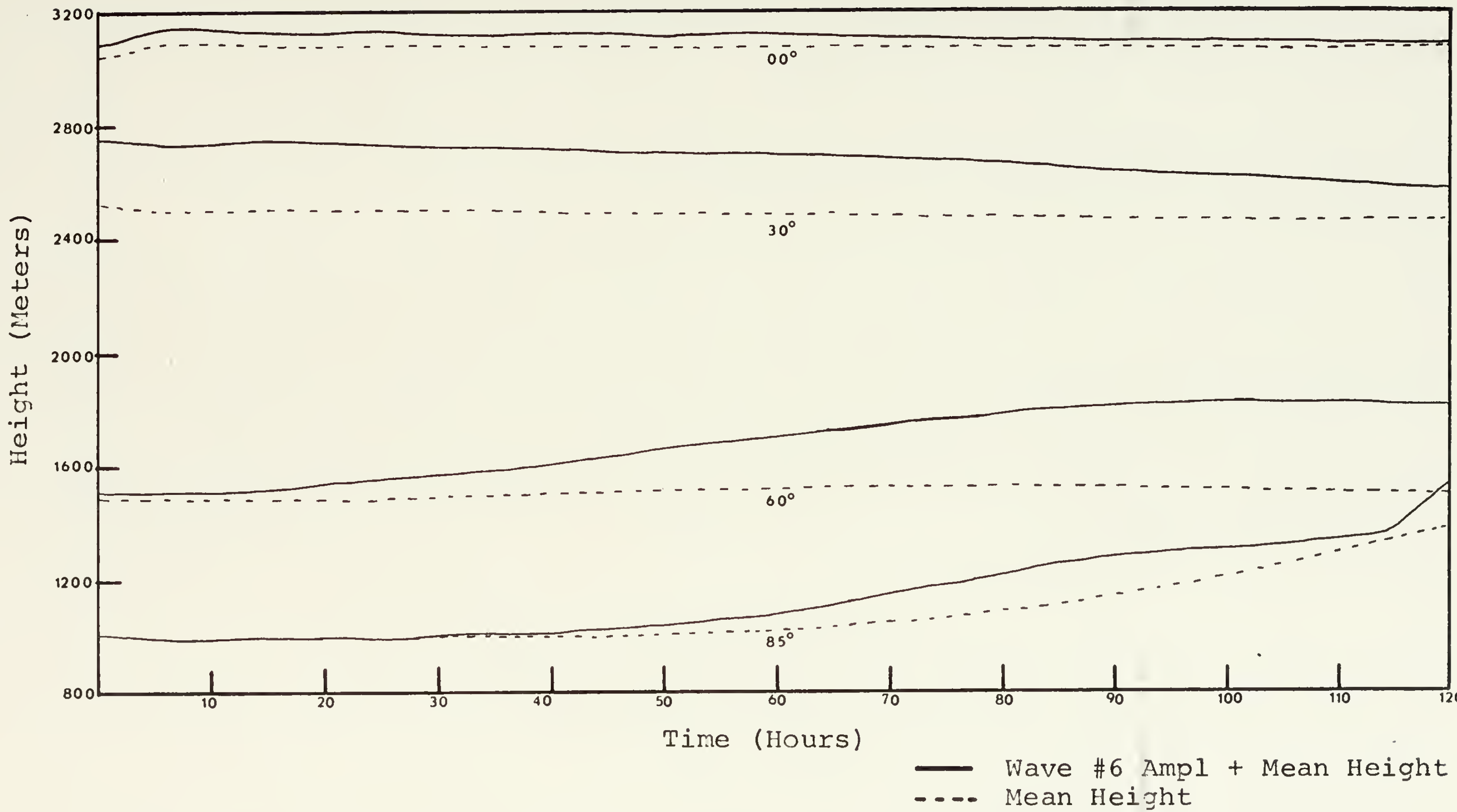

FIGURE 14. AMPLITUDE VS TIME FOR SELECTED LATITUDES USING THE EULER-BACKWARD SCHEME WITH AVERAGING.

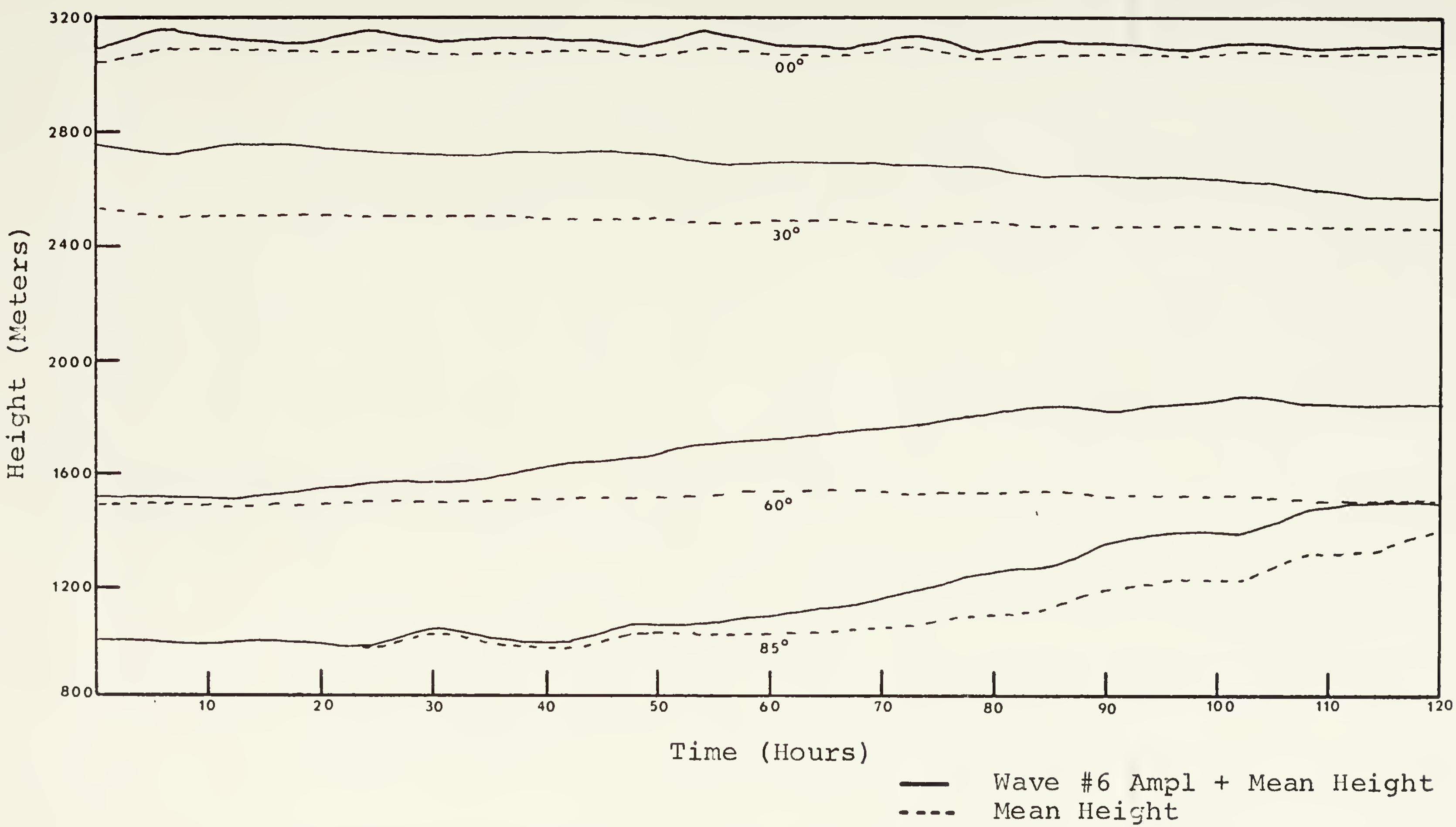

FIGURE 15. AMPLITUDE VS TIME FOR SELECTED LATITUDES USING THE LEAPFROG-TRAPEZOIDAL SCHEME WITH AVERAGING.

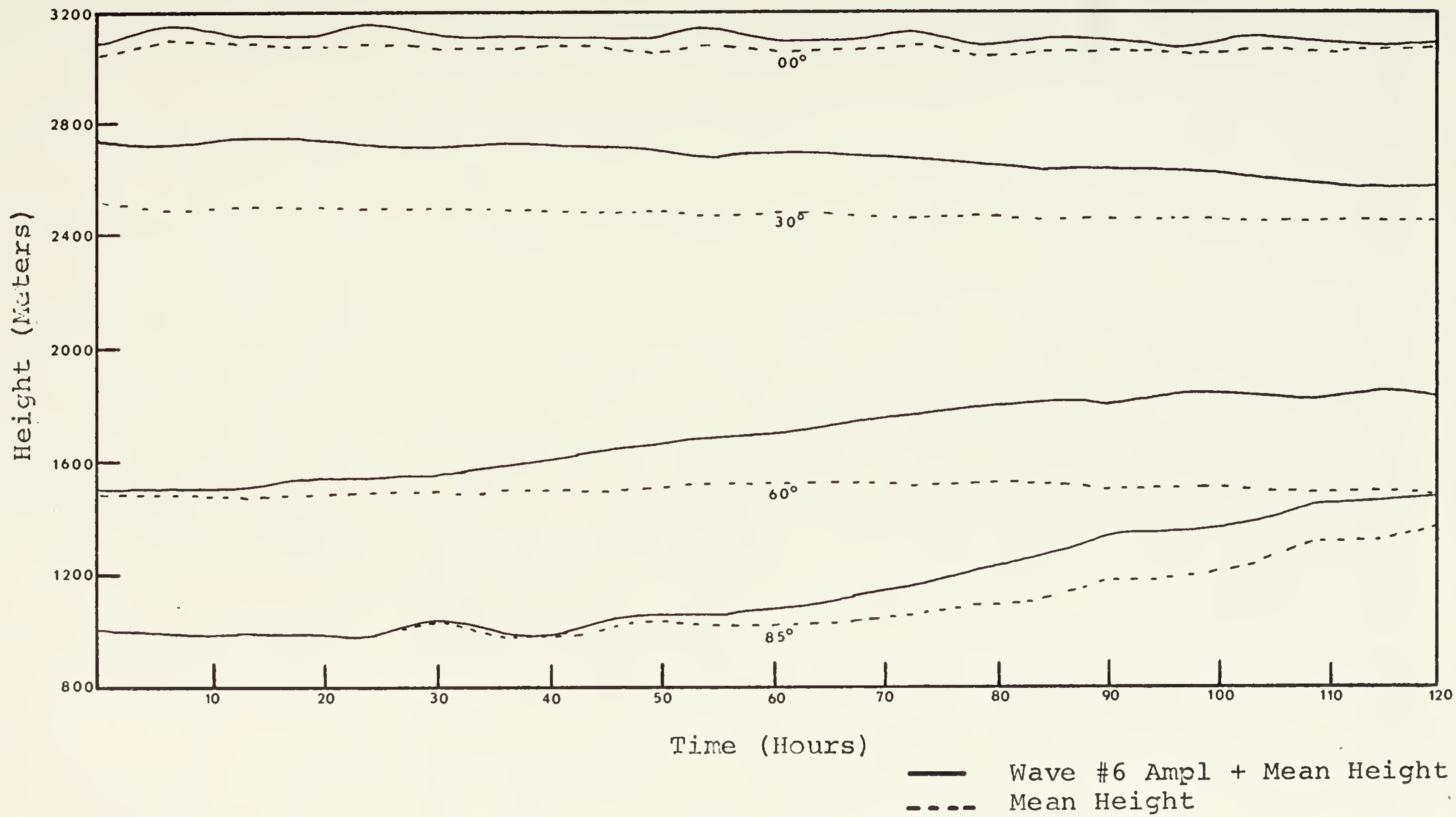

FIGURE 16. AMPLITUDE VS TIME FOR SELECTED LATITUDES USING THE ADAMS-BASHFORD SCHEME WITH AVERAGING.

VII. CONCLUSIONS

The Arakawa averaging method caused some problems with the initial field which was represented by a spherical harmonic, but it is felt that with real data, where the longitudinal scale does not necessarily decrease with latitude, the method might not cause such severe problems. Considering the alternatives, such as a reduced time step, variable grid size, or variable time step, the Arawaka procedure is a simple and effective method for spherical prediction. The reduced time step is much too expensive in computer time to be practical. The abruptly changed grid size causes severe problems around the area of the change. A variable time step might prove to be acceptable but would involve some very complex programming.

In the experiments performed, a second order one-dimensional interpolation was used since problems arose from using a two-dimensional linear interpolation and was the easiest to apply. In the real data cases, a two-dimensional second order interpolation scheme would probably give better overall results.

Overall the Euler-backward method gave the best results since it effectively reduced the amplitudes of the gravity waves, but was expensive in computer time. Considering time requirements and overall results, the leapfrog method is still the most desirable. Some further tests with combinations of the methods might produce a method which gives good results and is acceptable as far as time required is concerned.

BIBLIOGRAPHY

Arakawa, A., "Computational Design for Long-Term Numerical Integrations of the Equations of Atmospheric Motion," J. Computational Phys., v. 1, p. 119-143, 1966.

Gates, W. L, "On the Truncation Error, Stability and Convergence of Difference Solutions of the Barotropic Vorticity Equation," J. Meteor., v. 16, p. 556-568, 1959.

Gates, W. L., and Riegel, C. A., "A Study of Numerical Errors in the Integration of Barotropic Flow on a Spherical Grid," J. of Geoph. Res., v. 67, No. 2, p. 773-784, Feb. 1962.

Haltiner, G. J., Numerical Weather Prediction, p. 92-97 and 224-225, Wiley, 1971.

Lilly, D. K., "On the Computational Stability of Numerical Solutions of Time-Dependent Nonlinear Geophysical Fluid Dynamics Problems," Mon. Wea. Rev., v. 93, No. 1, p. 11-26, 1965.

Naval Postgraduate School Report NPS-51Wu71081A, Restorative-Iterative Initialization for a Global Prediction Model, by F. J. Winninghoff, September 1971.

Neamtan, S. M., "The Motion of Harmonic Waves in the Atmosphere," J. Meteor., v. 3, p. 53-56, 1946.

Rossby, C. G. and others, "Relation Between Variations in the Intensity of the Zonal Circulation of the Atmosphere and the Displacement of the Semi-Permanent Centers of Action," Journal of Marine Research, v. 2, p. 38-55, 1939.

UCLA Department of Meteorology Technical Report No. 3, Description of the Mintz-Arakawa Numerical General Circulation Model, by W. E. Langlois and C. W. Kwok, 1969.

INITIAL DISTRIBUTION LIST

		No. of Copies
1.	Defense Documentation Center Cameron Station Alexandria, Virginia 22314	2
2.	Library, Code 0212 Naval Postgraduate School Monterey, California 93940	2
3.	Dr. George J. Haltiner Chairman, Department of Meteorology Naval Postgraduate School Monterey, California 93940	5
4.	Associate Professor Roger T. Williams Code 51 Department of Meteorology Naval Postgraduate School Monterey, California 93940	5
5.	Lieutenant George W. Heburn FWC/JTWC COMNAVMAR Box 2 FPO San Francisco 96630	5
6.	Officer in Charge Environmental Prediction Research Facility Naval Postgraduate School Monterey, California 93940	1
7.	Commanding Officer U. S. Fleet Weather Central COMNAVMARIANAS, Box 12 FPO San Francisco 96630	1
8.	Commanding Officer Fleet Numerical Weather Central Naval Postgraduate School Monterey, California 93940	1
9.	ARCRL - Research Library L. G. Hanscom Field Attn: Nancy Davis/Stop 29 Bedford, Massachusetts 01730	1
10.	Director, Naval Research Laboratory Attn: Tech. Services Info. Officer Washington, D. C. 20390	1

11. American Meteorological Society 1
45 Beacon Street
Boston, Massachusetts 02128

12. Department of Meteorology 3
Code 51
Naval Postgraduate School
Monterey, California 93940

13. Department of Oceanography 1
Code 58
Naval Postgraduate School
Monterey, California 93940

14. Office of Naval Research 1
Department of the Navy
Washington, D. C. 20360

15. Commander, Air Weather Service 2
Military Airlift Command
U.S. Air Force
Scott Air Force Base, Illinois 62226

16. Atmospheric Sciences Library 1
National Oceanographic Atmospheric
Administration
Silver Spring, Maryland 20910

17. National Center for Atmospheric Research 1
Box 1470
Boulder, Colorado 80302

18. Dr. T. N. Krishnamurti 1
Department of Meteorology
Florida State University
Tallahassee, Florida 32306

19. Dr. Fred Shuman 1
Director
National Meteorological Center
Environmental Science Services
Administration
Suitland, Maryland 20390

20. Dr. J. Smagorinsky 1
Director
Geophysical Fluid Dynamics Laboratory
Princeton University
Princeton, New Jersey 08540

21. Dr. A. Arakawa 1
Department of Meteorology
UCLA
Los Angeles, California 90024

22. Professor N. A. Phillips 1
54-1422
M. I. T.
Cambridge, Massachusetts 02139

23. Dr. Russell Elsberry 1
Department of Meteorology
Naval Postgraduate School
Monterey, California 93940

24. Dr. Jerry D. Mahlman 1
Geophysical Fluid Dynamics Laboratory
Princeton University
Princeton, New Jersey 08540

25. Dr. Robert L. Haney 1
Department of Meteorology
Naval Postgraduate School
Monterey, California 93940

26. Dr. Ron L. Alberty 1
Department of Meteorology
Naval Postgraduate School
Monterey, California 93940

27. Dr. W. L. Gates 1
Department of Meteorology
Naval Postgraduate School
Monterey, California 93940

28. Dr. Richard Alexander 1
The Rand Corporation
1700 Main Street
Santa Monica, California 90406

29. Commanding Officer 1
Fleet Weather Central
Box 110
FPO San Francisco 96610

30. Dr. F. J. Winninghoff 1
Department of Meteorology
UCLA
Los Angeles, California 90024

31. LCDR P. G. Kessel 1
FNWC
Naval Postgraduate School
Monterey, California 93940

32. Mr. Leo C. Clarke 1
FNWC
Naval Postgraduate School
Monterey, California 93940

33. Naval Weather Service Command 1
Washington Navy Yard
Washington, D. C. 20390

Security Classification

DOCUMENT CONTROL DATA - R & D

(Security classification of title, body of abstract and indexing annotation must be entered when the overall report is classified)

ORIGINATING ACTIVITY (Corporate author) Naval Postgraduate School Monterey, California 93940	2a. REPORT SECURITY CLASSIFICATION Unclassified 2b. GROUP

REPORT TITLE

Numerical Experiments With Several Time Differencing Schemes With a Barotropic Primitive Equation Model on a Spherical Grid

DESCRIPTIVE NOTES (Type of report and, inclusive dates)

Master's Thesis; March 1972

AUTHOR(S) (First name, middle initial, last name)

George Washington Heburn

REPORT DATE	7a. TOTAL NO. OF PAGES	7b. NO. OF REFS
March 1972	49	9

CONTRACT OR GRANT NO.	9a. ORIGINATOR'S REPORT NUMBER(S)
PROJECT NO.	
	9b. OTHER REPORT NO(S) (Any other numbers that may be assigned this report)

DISTRIBUTION STATEMENT

Approved for public release; distribution unlimited.

SUPPLEMENTARY NOTES	12. SPONSORING MILITARY ACTIVITY Naval Postgraduate School Monterey, California 93940

ABSTRACT

Four time differencing schemes were tested using a barotropic primitive equation model on a spherical staggered grid with an analytic input in order to compare amplitudes, phase speeds, and computation time for each. The methods tested were the leapfrog, Euler-backward, leapfrog-trapezoidal, and Adams-Bashford. One set of experiments was performed using an averaging technique to reduce the effects of gravity waves in the higher latitudes. Another set was performed without the averaging in order to determine the effects of this technique on the solutions.

DD FORM 1 NOV 65 1473 (PAGE 1)

S/N 0101-807-6811

Security Classification

A-31408

14 KEY WORDS	LINK A		LINK B		LINK C	
	ROLE	WT	ROLE	WT	ROLE	WT
Barotropic Primitive Equation Model, Global						
Numerical Weather Prediction						
Time Differencing						
Spherical Grid						

Numerical experiments with several time differencing schemes with a barotropic primitive equation model on a spherical grid.

Thesis 133866
H4176 Heburn
c.1
Numerical experiments with several time differencing schemes with a barotropic primitive equation model on a spherical grid.